Endothelium-mediated action of analogs of the endogenous neuropeptide kyotorphin (Tyrosil-arginine): Mechanistic insights from permeation and effects on microcirculation.

Juliana Perazzo[§], Mônica Lopes-Ferreira[†], Sónia Sá Santos[§], Isa Serrano[§], Antónia Pinto[§], Carla Lima[†], Eduard Bardaji[‡], Isaura Tavares[#], Montserrat Heras[‡], Kátia Conceição[ϕ], Miguel A. R. B. Castanho[§]*.*

§- Instituto de Medicina Molecular, Faculdade de Medicina da Universidade de Lisboa, Av. Professor Egas Moniz, 1649-028 Lisboa, Portugal;

†- Unidade de Imunorregulação, Laboratório Especial de Toxinologia Aplicada, Instituto Butantan, Av. Vital Brasil 1500 São Paulo, Brazil;

‡- Laboratori d'Innovació en processos i Productes de Síntesi Orgànica (LIPPSO), Department de Química, Universitat de Girona, Campus Montilivi, 17071 Girona, Spain.

#- Instituto de Biologia Molecular e Celular, Porto, Portugal; i3S - Instituto de Inovação e Investigação em Saúde, Universidade do Porto, Porto, Portugal; Departamento de Biologia Experimental, Faculdade de Medicina, Universidade do Porto, Portugal.

ϕ- Departamento de Ciências e Tecnologia, Universidade Federal de São Paulo, UNIFESP, Rua Talim, 330, São José dos Campos, Brazil.

KEYWORDS: Kyotophin, analgesia, microcirculation, permeability, pain, blood-brain barrier

ABSTRACT

Kyotorphin (KTP) is an endogenous peptide with analgesic properties when administered into the central nervous system (CNS). Its amidated form (L-Tyr-L-Arg-NH_2; KTP-NH_2) has improved analgesic efficacy after systemic administration, suggesting blood-brain barrier (BBB) crossing. KTP-NH_2 also has anti-inflammatory action impacting on microcirculation. In this work, selected derivatives of KTP-NH_2 were synthesized to improve lipophilicity and resistance to enzymatic degradation while introducing only minor changes in the chemical structure: N-terminal methylation and/or use of D amino acid residues.

Intravital microscopy data show that KTP-NH_2 having a D-Tyr residue, KTP-NH_2-DL, efficiently decreases the number of leukocyte rolling in a murine model of inflammation induced by bacterial lipopolysaccharide (LPS): down to 46% after 30 min with 96 μM KTP-NH_2-DL. The same molecule has lower ability to permeate membranes (relative permeability of 0.38) and no significant activity in a behavioral test which evaluates thermal nociception (hot-plate test). On the contrary, methylated isomers at 96 μM increase leukocyte rolling up to nearly 5-fold after 30 min suggesting a pro-inflammatory activity. They have maximal ability to permeate membranes (relative permeability of 0.8) and induce long-lasting antinociception.

1. INTRODUCTION

Kyotorphin is a small endogenous dipeptide, L-Tyr-L-Arg (KTP), firstly isolated from a bovine brain in 1979[1-2] and afterwards localized in the brain synaptosomes of mammals[3]. KTP is a powerful neuropeptide being four-fold more potent than endogenous opioids;[1] however, the remarkable antinociceptive action of KTP in animal models was observed only when the molecule was administered directly into the CNS.[4] The reduced ability of KTP to cross the blood-brain barrier (BBB) is the most accepted explanation.[5] The analgesia induced by KTP appears to be opioid-mediated via the release of the opioid Met-enkephalin involved in pain control.[1, 6-7] It is suggested that KTP also mediates non-opioid activity without the release of enkephalins.[8-9]

Recently we have found that amidated KTP (KTP-NH_2) causes analgesia after systemic administration, which suggests KTP-NH_2 is able to cross the BBB[10], in spite of modest permeation through lipid membranes.[11] In addition, KTP levels in cerebro-spinal fluid correlate negatively with the progression of neurodegeneration in Alzheimer's Disease patients[12] and KTP-NH_2 has neuroprotective effects in an animal model of dementia[13]. Because recent evidence shows that Alzheimer's Disease is primarily a vascular disease with neurodegenerative consequences, rather than a neurodegenerative disorder with vascular consequences,[14] and the activity of KTP-NH_2 at BBB level, we have raised the hypothesis that the endothelium is a key element in the pharmacological action of KTP-NH_2. In addition to its hypothetical endothelial targeting, KTP-NH_2 is also an appealing drug lead because it does not cause damage on microcirculation,[15] has no significant cytotoxic effects[10] and does not induce the side effects associated to opioid drugs.[16] When covalently associated to ibuprofen, KTP-NH_2 enhances the anti-inflammatory action of ibuprofen[15] and the ibuprofen moiety enhances the analgesic action of KTP-NH_2.[17] Chemical manipulation of KTP-NH_2 is a strategy to modulate its action. The key

elements of KTP-NH_2 chemical nature that interfere with its biological action are the cationic charge[18], lipophilicity[19] and resistance to enzymatic degradation.[10, 17] In this study we have pursued the goal of finding simple and inexpensive KTP-NH_2 derivatives having endothelium-mediated action both as analgesic and anti-inflammatory drugs. The strategy was to explore enantiomers of KTP-NH_2 by using D-Tyr and/or D-Arg residues and/or methylation capping at the N-terminus. All the derivatives are thus analogs of KTP-NH_2 with minimal differences in structure, while exploring variation in charge, lipophilicity and resistance to peptidases. An integrated approach using in vivo data from intravital microscopy (IVM) and evaluation of thermal nociceptive responses in rodents, combined with mechanistic permeation data in vitro, was used to unravel new drug leads targeted to endothelium-mediated action with impact both in inflammation and analgesia.

2. RESULTS

2.1. Synthesis of kyotorphin derivatives

First, amidated kyotorphin derivatives H-D-Tyr-Arg-NH_2 (KTP-NH_2-DL), H-Tyr-D-Arg-NH_2 (KTP-NH_2-LD), H-D-Tyr-D-Arg-NH_2 (KTP-NH_2-DD), H-N-Me-Tyr-D-Arg (Me-KTP-NH_2-LD) and H-N-Me-Tyr-Arg (Me-KTP-NH_2) have been prepared in small scale through standard solid phase peptide synthesis using a 9-fluorenylmethoxycarbonyl (Fmoc) / *tert*-butyl (*t*-Bu) strategy as illustrated in Scheme 1. Key elements of this solid-phase peptide synthesis are, employment of *t*-Bu group and 2,2,5,7,8-pentamethyl-chroman-6-sulfonyl (pmc) group as masks for the side chains of tyrosine and arginine, respectively; removal of Fmoc groups by treatment with 30% piperidine in dimethylformamide (DMF) and amide couplings mediated by *O*-(benzotriazol-1-yl)-*N*,*N*,*N*',*N'*-tetramethyluronium hexafluorophosphate (HBTU) in the

presence of *N*-hydroxybenzotriazole (HOBt) as racemization suppressant and diisopropylethylamine (DIEA) as base.

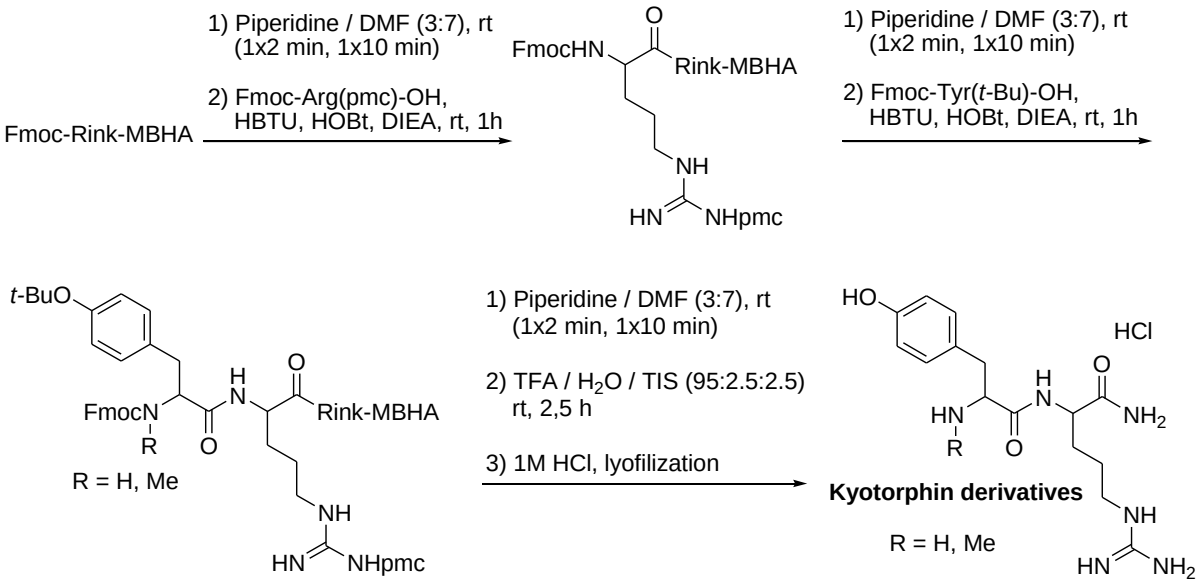

Scheme 1. General synthetic route for solid phase synthesis of kyotorphin derivatives.

The side chain protection of arginine is an unsolved problem in solid phase peptide synthesis because the usually employed arylsulfonyl-based protecting groups (e.g. pmc)[20] are too stable to TFA and need extended cleavage to complete removal during the release step of the peptide from the support.[21] In addition, sometimes they are also difficult to scavenge and have a tendency to reattach or alkylate sensitive residues. Knowing this, the release step of KTP-NH_2-DL peptide was first examined using three different cleavage cocktails (Table 1). Reagents R[22] and B[23] are the most recommended cleavage cocktails for those peptides containing, among others amino acids residues, Arg(pmc). Nevertheless, under these conditions KTP-NH_2-DL was obtained in poor purity together with a significant amount of peptide with arginine residue still pmc-protected KTP-NH_2-DL(pmc) and several no identified impurities (Table 1, entries 1 and 2). The standard mixture of cleavage with TFA, water and triisopropylsilane (TIS) was tested at different cleavage times (Table 1, entries 3-6). After 2:20 hours treatment,

acceptable results of 80% purity of KTP-NH_2-DL and only a 2% of KTP-NH_2-DL(pmc) were obtained (Table 1, entry 5). Increasing cleavage time provided worse results (Table 1, entry 6). The best cleavage conditions were applied to the others kyotorphin derivatives which were obtained in a range of purities of 72-87%.

Next, the crude kyotorphin derivatives were purified manually by reverse-phase flash chromatography and the pure peptides obtained were dissolved in 1M aqueous HCl and lyophilized for three times to afford kyotorphin derivatives as a hydrochloride salts, with final yields and purities shown in Table 2.

Table 1. KTP-NH_2-DL peptide submitted to different cleavage conditions

Entry	Cleavage cocktail	Time (h)	KTP-NH_2-DL (%)[c]	KTP-NH_2-DL(pmc) (%)[c]
1	TFA / thioanisole / EDT / anisole[a] (90:5:3:2)	2:00	55	3
2	TFA / phenol / H_2O / TIS[b] (88:5:5:2)	3:00	35	50
3	TFA / TIS / H_2O (95:2.5:2.5)	2:00	50	11
4	TFA / TIS / H_2O (95:2.5:2.5)	2:15	67	13
5	TFA / TIS / H_2O (95:2.5:2.5)	2:25	80	2
6	TFA / TIS / H_2O (95:2.5:2.5)	4:00	42	25

[a]Reagent R. [b]Reagent B. [c]Percentage determined by HPLC at 220 nm from the crude peptide.

Table 2. Yields and purities of kyototphin derivatives synthesized in solid phase

Reference	Sequence	Yield (%)[a]	Purity (%)[b]	HPLC t_R (min)
KTP-NH_2-DL	H-D-Tyr-Arg-NH_2	52	99.9	2.35
KTP-NH_2-LD	H-Tyr-D-Arg-NH_2	70	98.2	2.41
KTP-NH_2-DD	H-D-Tyr-D-Arg-NH_2	80	99.9	1.52
Me-KTP-NH_2-LD	H-N-Me-Tyr-D-Arg-NH_2	60	97.7	2.28
Me-KTP-NH_2	H-N-Me-Tyr-Arg-NH_2	58	98.7	1.66

[a]Yields were calculated from isolated product after reverse-phase flash chromatography. [b]Percentage determined by HPLC at 220 nm from the crude peptide.

Lead kyotorphin derivatives KTP-NH_2-DL, Me-KTP-NH_2-LD and Me-KTP-NH_2 have been prepared in large scale through standard solution phase peptide synthesis as illustrated in Scheme 2. Boc-Tyrosine building block are commercial available protected with benzyl (Bzl) group in the side chain. Amide coupling between tyrosine and arginine building blocks was mediated by benzotriazole-1-yl-oxy-tris-(dimethylamino)-phosphonium hexafluorophosphate (BOP) in the presence of *N*-methylmorpholine (NMM) at room temperature. Under these conditions all protected kyotorphin derivatives were obtained in moderate to good yields and in excellent purities (Scheme 2).

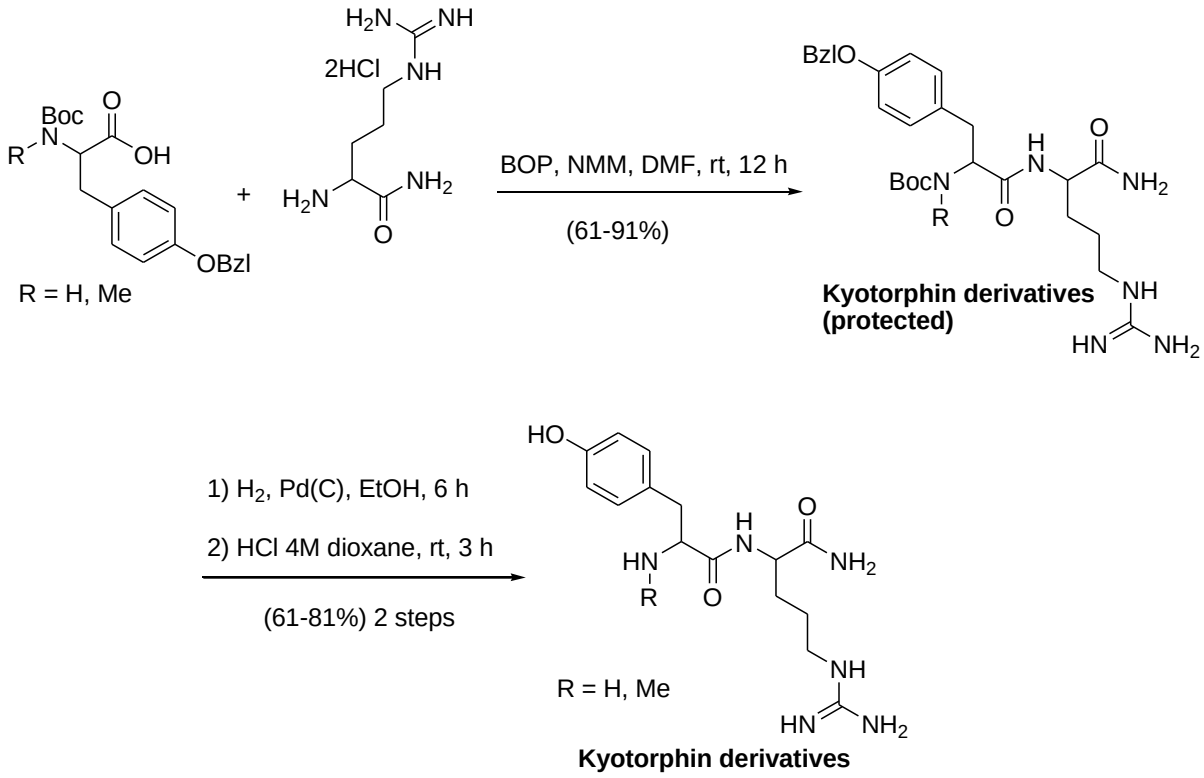

Scheme 2. Solution phase synthesis of kyotorphin derivatives

In the case of methylated derivatives although a single peak by HPLC analysis was observed, its ^{1}H NMR spectra showed some protons split specially for the α-carbonylic protons. In order to distinguish between a conformational equilibrium and a possible epimerization occurred during coupling reaction, a variable-temperature ^{1}H NMR study was undertaken. At 20 ºC the α-carboxylic protons of Me-KTP-NH_2-LD (protected) exhibit two separate and broad singlet signals, which coalesce between 40-60 ºC (Figure 1), and sharpen even more at higher temperatures. These results are unequivocal evidence that the methylated kyotorphin derivatives present a slow conformational equilibrium which can be observed on the NMR time scale, and that epimerization process does not take place during coupling reaction.

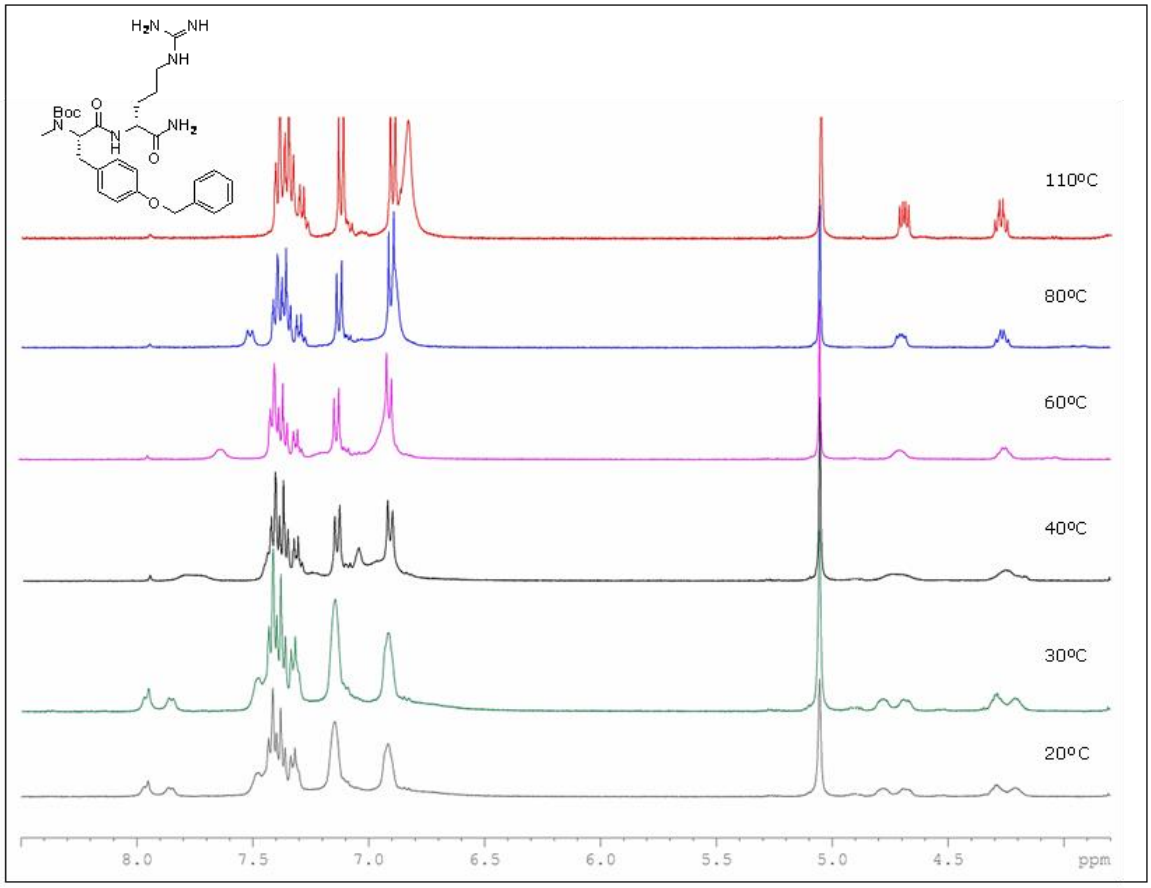

Figure 1. ^{1}H NMR spectra (region 4-8.5 ppm) of Me-KTP-NH_2-DL (protected) recorded in DMSO-*d*6 from 20 to 110 ºC

Next, Bzl and Boc protecting groups of the kyotorphin derivatives, were removed by catalytic hydrogenation and treatment with a 4M solution of HCl in dioxane respectively. Thus, the final kyotorphin derivatives were obtained as hydrochloride salt in good yields (Scheme 2).

2.2. Selection of lead compounds based on lipid interaction and serum stability

KTP-NH_2 is unstable in human serum (90% conversion in free amino acids after 60 min by HPLC), KTP-NH_2-LD is relatively stable (20% conversion), and the other derivatives are very stable (less than 10% conversion). Lipid interaction studies[21] using anionic lipids to better mimic brain endothelium surface[15] has shown a stronger

interaction of the derivatives KTP-NH_2-DL, Me-KTP-NH_2-LD, and Me-KTP-NH_2 with lipid membranes (Figure 2), indicative of an increased potential to translocate membranes as insertion on lipid bilayers is the first key event in diffusion across membranes or receptor targeting. [21] Compounds KTP-NH_2-DL, Me-KTP-NH_2-LD, and Me-KTP-NH_2 are the most promising both in terms of pharmacokinetics (stability in serum) and efficacy (potential to translocate the blood-brain barrier) and were therefore selected as lead compounds in this study.

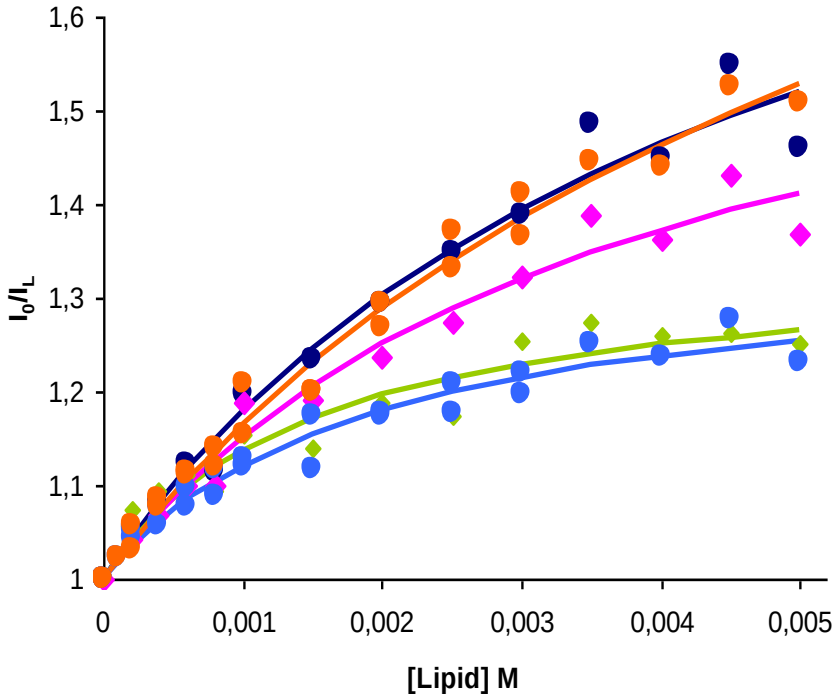

Figure 2: Normalized Tyr residue fluorescence emission upon titration of the KTP derivatives with lipid vesicles of POPG [1-hexadecanoyl-2-(9Z-octadecenoyl)-*sn*-glycero-3-phospho-(1'-*rac*-glycerol)], as described in references 21 and 14. Maximal deviation from the initial value of fluorescence intensity reflects how strongly the fluorescence quantum yield of Tyr residue is affected by contact with the lipid. KTP-NH_2-LD – Light blue; KTP-NH_2-DL - pink, KTP-NH_2-DD – green, Me-KTP-NH_2-LD – Dark blue, and Me-KTP-NH_2 – Orange.

2.3. Intravital microscopy studies

Changes in the dynamics of microcirculation were evaluated by intravital microscopy following topical application of 20 μL of KTP derivatives 48 or 96 μM to mice cremaster muscle. Despite structural similarities, KTP derivatives presented distinct alterations in microcirculation. The peptide Me-KTP-NH_2 increased hugely the number of rolling leukocytes in a concentration-dependent manner. Except that at 10 min, 48 μM of this peptide increased more leukocyte rolling than 96 μM ($p < 0.001$). These values remained high, statistically unchanged, at 20 and 30 min (Figure 3A). The increase of rolling leukocytes caused by 48 μM of Me-KTP-NH_2 was about 4 fold compared to basal values ($p < 0.001$). At the highest concentration tested of 96 μM, Me-KTP-NH_2 increased approximately 6 fold the leukocyte rolling compared to control and reached a plateau at 20 min (Figure 3A). Moreover, a transient arteriolar contraction was observed 10 min after topical application of 96 μM Me-KTP-NH_2 (Figure 3C), while lower concentration caused an arteriolar contraction in only 25% of tested animals. No adherent leukocytes were observed over the experiment (data not shown). The peptide Me-KTP-NH_2-LD did not show a concentration-dependent behavior, but also increased leukocyte rolling, by approximately 3 fold (Figure 3A). Furthermore, Me-KTP-NH_2-LD isomer did not induce arteriolar contraction nor increased the number of adherent leukocytes (data not shown). However, both Me-KTP-NH_2-LD and Me-KTP-NH_2 showed pro-inflammatory properties.

In contrast, KTP-NH_2-DL did not increase leukocyte rolling (Figure 3A). Consequently, we decided to study its effects on LPS-induced inflammation model. Mice injected ip with 0.05 μg/kg LPS present an average of 75 rolling leukocytes per min along the

vessel wall. Topical treatment with KTP-NH_2-DL reduced that number to approximately 39 rolling leukocytes per min. This result evidence a potential role of this isomer as an anti-inflammatory compound.

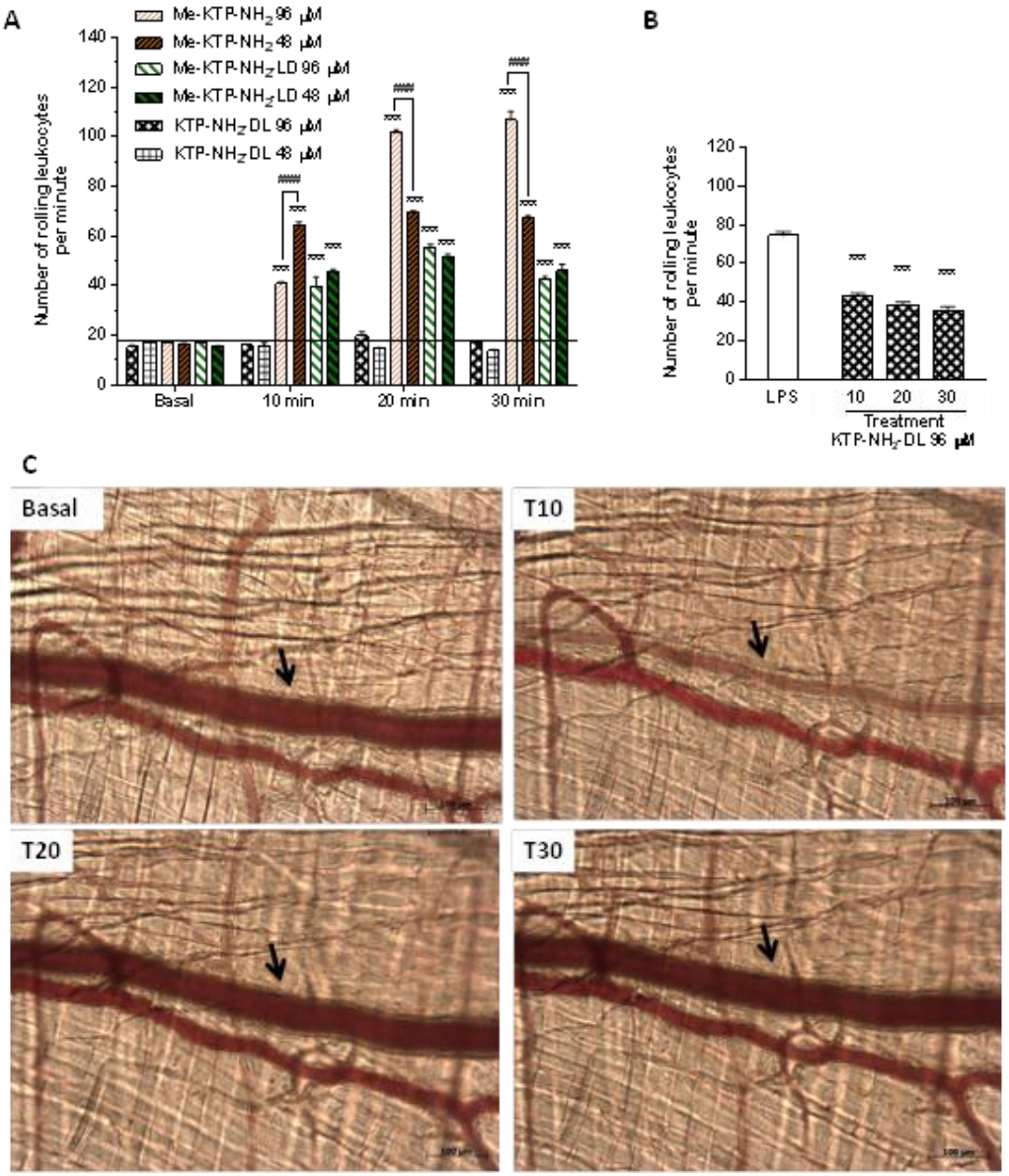

Figure 3. Effects of KTP-NH_2 derivatives on microcirculation. (A) Number of rolling leukocytes per minute after topical application of 48 or 96 µM of the KTP-NH_2-DL, Me-KTP-NH_2 and Me-KTP-NH_2-LD peptides on the mice cremaster muscle ($n \geq 4$) at different time points. Bars represent mean ± SEM. Basal values correspond to number of rolling leukocytes per minute before peptide application. The horizontal line

represents the average number of rolling leukocytes over time after PBS application. *** $p < 0.001$ compared to PBS using two way ANOVA followed by Tukey's post test, ### $p < 0.001$. (B) Number of rolling leukocytes per minute after challenge with LPS (0.05 μg/kg, ip) and following topical treatment with 96 μM of KTP-NH_2-DL. Determinations were performed each 10 min up to 30 min after peptide topical application on the mice cremaster muscle (n = 4). Each point represents mean ± SEM. ***$p<0.001$ compared with LPS (control group: topical application of PBS) using two-way ANOVA followed by Tukey's post test; (C) Transient arteriolar contraction at 10 min after Me-KTP-NH2 (96 μM) topical application.

2.4. Evaluation of thermal nociceptive responses

The analgesic effects of Me-KTP-NH2-LD and Me-KTP-NH2 were evaluated after ip administration to male Wistar rats. Both peptides induced a dose- and time-independent increased response threshold (average variation of 2-2.6ºC in relation to the respective baseline levels). In fact, after injection of Me-KTP-NH2-LD at either 50 μmol/kg or 96 μmol/kg increases in threshold were detected at all timepoints, except at 75 minutes ($p<0.05$ at 30 and 90 minutes and $p<0.01$ at 15, 45 and 60 minutes for the dose 50 μmol/kg; $p<0.05$ at 90 minutes, $p<0.01$ at 30 and 60 minutes and $p<0.001$ at 15 and 45 minutes for the dose 96 μmol/kg; Figure 4). Regarding the injection of Me-KTP-NH2 at 50 μmol/kg an increase in threshold was detected 15 ($p<0.01$) and 45 minutes post-injection ($p<0.05$). With the 96μmol/kg the increases were detected at all the timepoints, except at 75 minutes ($p<0.05$ at 30, 60 and 90 minutes and $p<0.01$ at 15 and 45 minutes; Figure 4). After injection with saline, the variations in relation to the respective baseline levels along the time were negligible or nil (Figure 4). Regarding the effects of the peptide KTP-NH2-DL, statistically significant increases were only

detected at 45 minutes with the dose of 50 µmol/kg (Figure 4). Overall, the results indicate an analgesic effect of both LL and LD Me-KTP-NH2 isomers, whereas the peptide KTP-NH2-DL did not show a relevant analgesic effect.

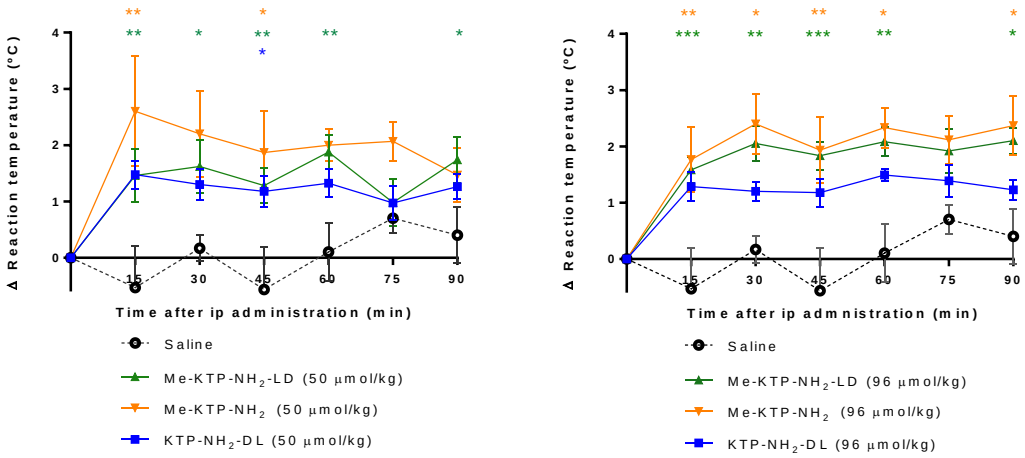

Figure 4. Effect of KTP-NH_2 derivatives on the nociceptive threshold of rats in the hot-plate test. Results shown as the difference between responses at each time point relative to basal values (time zero, i.e. immediately before injection). Compounds were ip administered at 50 µmol/kg (left panel) or 96 µmol/kg (right panel). Each point represents mean ± SEM (n≥5). *** $p < 0.001$, ** $p < 0.01$ and * $p < 0.05$ versus saline-treated animals using two way ANOVA followed by Tukey's post test.

2.5. Permeation studies with drug candidates

The time-dependence of the normalized fluorescence emission intensity of the drugs in covered and blank filters versus time is presented in Supporting information (Figure S1). The relative permeability was calculated for each drug candidate (Figure 5). The

PR of the five peptides ranged from 0.38 to 0.81, the highest value being attained by Me-KTP-NH_2. The P_R of KTP-NH_2-DL was significantly inferior to the one of KTP.

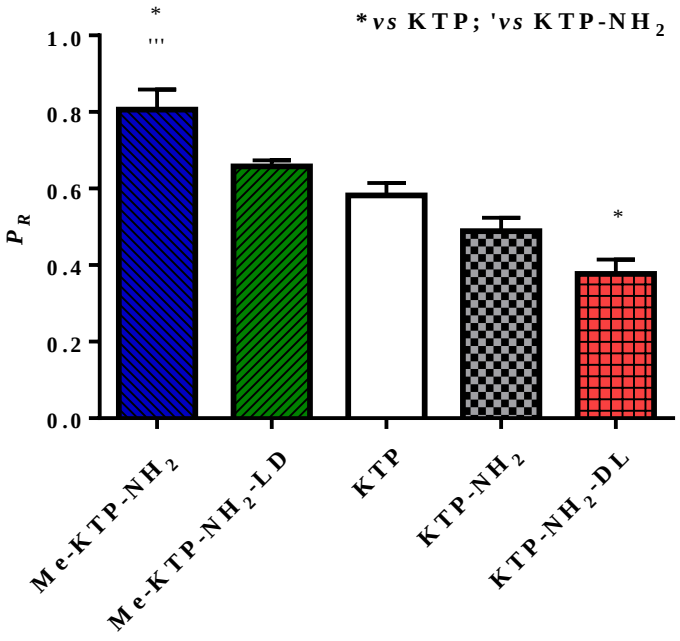

Figure 5. Relative permeability of Me-KTP-NH_2, Me-KTP-NH_2-LD, KTP-NH_2-DL, KTP, and KTP-NH_2. Data showed as mean ± SEM; each group is an average of three independent measures. *P < 0.05 versus KTP; '"P < 0.001 versus KTP-NH_2. One-way ANOVA, followed by Tukey's post test.

3. DISCUSSION

A new series of KTP-NH_2 derivatives have been designed in order to improve endothelial targeting both at peripheral and BBB level and were evaluated for their impact on microcirculation and analgesic efficacy in vivo. The potential to transpose lipid membranes in vitro was also evaluated. Modifications consisted in N-terminal methylation and/or L to D amino acid change.

The evaluation of the microcirculatory environment was assessed through IVM. This technique have been used for decades to help scientists understand the biophysical

conditions under which leukocytes are exposed to in microvessels [24-26]. IVM provides a tool to acquire quantitative, qualitative, and dynamic insights into cell biology and endothelial-leukocyte interactions relevant to understanding the pathophysiology of inflammation in different disease states [27].

After KTP derivatives application, the microcirculatory environment did not reveal toxic effects such as thrombi formation or contraction of myofibrils, however Me-KTP-NH_2 and Me-KTP-NH_2-LD increased 6 and 3 fold, respectively, the number of rolling leukocytes relative to control (Figure 3), revealing a potential pro-inflammatory effect. However, vasodilatation, one of the earliest events of acute inflammation, was not detected. On the contrary, KTP-NH_2-DL did not increase leukocyte rolling nor induced cellular recruitment. In addition, it decreased leukocyte rolling induced by LPS (Figure 3B). This endotoxin is found in the outer membrane of Gram-negative bacteria and once LPS reaches the blood flow, it activates the CD14/toll-like receptor 4 (TLR4)/myeloid differentiation protein 2 (MD2) complex on the surface of immune cells consequently promoting the secretion of pro-inflammatory cytokines, nitric oxide, eicosanoids and inducing neutrophils recruitment.

KTP-NH_2-DL has low permeation across lipid membranes as P_R = 0.4 (Figure 5), a value at which no significant analgesic effect is expected among KTP derivatives that diffuse across lipid bilayers.[19] Consistently, KTP-NH_2-DL has the lowest analgesic effect among the three lead drugs tested (Figure 4). KTP-NH_2 is more effective than expected from simple inference based on PR[19] but KTP-NH_2-DL does not retain this property. As previously suggested[19], KTP-NH_2 probably uses an active transporter like peptide transporter 2 (PEPT2) to translocate the BBB. Data in Figure 3 corroborates this hypothesis as KTP-NH_2-DL is an diastereoisomer of KTP-NH_2 and completely loses efficacy. The data suggest that KTP-NH_2 derivatives having high PR permeate through

the BBB passively and cause analgesia while KTP-NH_2 uses a selective transporter. This hypothesis also explains why KTP-NH_2 has a fast transient effect while methylated (Figure 5) and other derivatives have prolonged effects:[10, 17] derivatization in both endings such as amidation at C terminus and methylation at N terminus, protects the peptides from the action of peptidases and proteases, improving pharmacokinetics. Me-KTP-NH_2 is highly permeable having $P_R = 0.8$. The addition of a neutral, hydrophobic methyl group to KTP-NH_2 was a significant step to improve the interaction with lipid and confer increased membrane permeation. We have previously described a direct correlation between membrane permeation and analgesic activity.[19] The data obtained in the hot-plate test corroborate this hypothesis. The analogs with higher PR, Me-KTP-NH_2 and Me-KTP-NH_2-LD, are the most effective in analgesia (Figure 4).

In this study we have discovered KTP-NH_2-DL, an anti-inflammatory drug lead, and Me-KTP-NH_2, a very effective membrane-translocator analgesic drug lead. The parent molecule KTP-NH_2 combines anti-inflammatory properties with analgesic efficacy. Isomerization of the Tyr residue (D-Tyr) decreases permeation through membranes and abrogates analgesic action. Methylation at the N terminus increases permeation and improves analgesic efficacy but abrogates anti-inflammatory action, probably a consequence of cell-penetration at the endothelium and/or blood cells. Since the hot-plate is a behavioral test that evaluates acute responses to thermal nociceptive stimulation and in which the inflammatory reaction is nil[32], future studies will evaluate the effects of those analogs in inflammatory pain models, such as articular inflammation.

The mechanism of action of KTP-NH_2 is still not totally clarified but the dual effect of KTP-NH_2[15] in pain and inflammation might shed light on this matter. Ueda and co-workers suggested that KTP receptor is coupled to G_i protein and mediates calcium

influx via phospholipase C (PLC).[28] PLC also plays an important role in the inflammation pathway catalyzing the release of arachidonic acid that subsequently promotes the release of prostaglandins and leukotrienes. It is reasonable to speculate that KTP-NH_2 might interact with G protein coupled receptors that play a role simultaneously in pain and inflammation. A good hypothetic target would be the protease-activated receptors (PARs). They are widely distributed in a variety of tissues and can be activated by small peptides, triggering different intracellular pathway depending on the cell type. "PARs are in essence peptides receptors that carry their own ligand, which remain silent until unmasked by site-specific receptor cleavage".[29] Four PAR isoforms have been identified so far. PAR1 and PAR4 agonists are able to induce analgesia and inflammation, while PAR2 antagonist cause analgesia and are anti-inflammatory. The interaction of KTP-NH_2 with PARs could be the key to explain how KTP-NH_2 and its derivatives impact on inflammation and analgesia.

4. CONCLUSIONS

1) KTP-NH_2 is anti-inflammatory in mice as revealed by IVM and analgesic in rats as revealed by the hot plate test. Methylation at the N terminus enhances analgesic efficacy through increased permeation across lipid membranes but abrogates anti-inflammatory action. Isomerization of the L-Tyr residue has the opposite effect.

2) Globally, the results support the hypothesis that KTP-NH_2 uses a specific transporter across the BBB, not fitted to transport KTP-NH_2 derivatives. Methylated derivatives permeate membranes passively and may diffuse across the BBB, thus compensating for the lack of activity of the transporter.

3) KTP-NH_2-DL has a pronounced anti-inflammatory action but low permeation through lipid membranes and decreased analgesic action.

In addition, the study opens new perspectives by casting the hypothesis that the interference of KTP-NH_2 and its derivatives with PAR may be the key to understand the dual action of these drugs in inflammation and nociception. PARs are expressed in endothelial cells and neurons, besides platelets and myocytes.

5. EXPERIMENTAL SECTION

5.1. Peptide synthesis

General Synthetic Procedures. KTP and KTP-NH_2 were synthesized as described before.[10] All chemicals used for peptide synthesis were purchased from Sigma-Aldrich, Fluka, Bachem or Iris-Biotech and used without further purification. The peptides synthesized in solid-phase were analyzed for purity on high performance liquid chromatography (HPLC) and characterized by mass spectra under electrospray ionization (ESI-MS) and proton nuclear magnetic resonance (^{1}H-NMR). The peptides synthesized in solution phase were analyzed for purity on HPLC and characterized by ^{1}H-NMR, carbon nuclear magnetic resonance (^{13}C NMR) and high resolution mass spectra under electrospray ionization (HRMS-ESI). HPLC analyses were carried out using a Dionex instrument composed of an UV/Vis Dionex UVD170U detector, a P680 Dionex bomb, an ASI-100 Dionex automatic injector, and CHROMELEON™ 6.60 software. Separations were achieved on an analytical 100-C_{18} Kromasil reversed phase column (4.6 mm x 40 mm; 3.5 μm particle size). The compounds were eluted using a linear gradient of 0–100% CH_3CN in 0.1% TFA at flow rate of 1.0 mL/min. The absorbance was measured at 220 nm. The HPLC retention time of each compound was determined when the peak was at its maximum height. NMR spectra were recorded at 400 MHz on a Brucker DPX Advance spectrometer. Spectra recorded in DMSO-d_6 were referenced to residual DMSO-d_6 at 2.50 ppm for ^{1}H or 39.5 ppm for ^{13}C. Spectra

recorded in D_2O were referenced to 4,4-dimethyl-4-silapentane-1-sulfonic acid (DDS = 0.0 ppm) as an internal standard. Coupling constants (*J*) are given in Hertz (Hz). The following abbreviations were used for spin multiplicity: s = singlet, d = doblet, t = triplet, q = quarter, m = multiplet, dd = double doublet, bs = broad singlet. ESI-MS analyses were performed with an Esquire 6000 ESI ion Trap LC/MS (Bruker Daltonics) instrument equipped with an electrospray ion source. The instrument was operated in the positive ESI(+) ion mode. Samples (5 μL) were introduced into the mass spectrometer ion source directly through an HPLC autosampler. The mobile phase (80:20 CH_3CN/H_2O at a flow rate of 100 μLmin–1) was delivered by a 1100 Series HPLC pump (Agilent). Nitrogen was employed as both the drying and nebulising gas. HRMS were recorded under conditions of ESI with a Bruker MicroTof-Q instrument using a hybrid quadrupole time-of-flight mass spectrometer (University of Zaragoza). Samples were introduced into the mass spectrometer ion source directly through a 1100 Series Agilent HPLC autosampler and were externally calibrated using sodium formate. The instrument was operated in the positive ESI(+) ion mode. Reverse-phase flash chromatography (RF-FC) purifications were performed manually on C_{18}-reverse-phase silica gel 100 (400 mesh, Fluka).

5.1.1. Solid phase synthesis of peptides KTP-NH_2-DL, KTP-NH_2-LD, KTP-NH_2-DD, Me-KTP-NH_2-LD and Me-KTP-NH_2.

General procedure. Peptides were prepared manually by the solid-phase method using Fmoc-type chemistry, Fmoc-Rink-MBHA resin (0.56 mmol/g) as solid support, *tert*-butyl side chain protection for tyrosine and pmc for arginine. Coupling of amino acids was mediated by a mixture of HBTU (3.8 equiv), HOBt (4 equiv), and DIEA (3 equiv) in DMF at room temperature for 1 hour. The completion of the reactions was monitored

by the Kaiser test. Fmoc group was removed by treating the resin with 30% piperidine in DMF (2 + 8 min). After each coupling and deprotection step, the resin was washed with DMF (6 x 1 min) and air-dried. A mixture of TFA, water and TIS was used as cleavage cocktail.

The Fmoc-Rink-MBHA resin (450 mg) was placed into a plastic syringe fitted with a polypropylene frit to remove the Fmoc group and subsequently couple with arginine amino acid (4 equiv). After Fmoc group removal the resin was treated with tyrosine derivative (4 equiv). The resulting dipeptides were deprotected with piperidine and released from the solid support by treatment with TFA/H_2O/TIS (95:2.5:2.5) with stirring for 2.25 h at room temperature. Following TFA evaporation and diethyl ether extraction, the crude peptides were purified by reverse-phase flash chromatography (H_2O/MeOH/TFA 90:10:0.01%). The resulting white solid was dissolved in 1M aqueous HCl and lyophilized. This process was repeated three times to afford kyotorphin derivatives as a hydrochloride salt.

KTP-NH_2-DL. By the general procedure, Fmoc-Arg(pmc)-OH (4 equiv) and Fmoc-D-Tyr(*t*Bu)-OH (4 equiv) provided H-D-Tyr-Arg-NH_2 (48 mg, 52%) as a colorless solid. HPLC (water/acetonitrile, 0.1% TFA, 2-100%, 17 min): retention time, 2.36 min; 99.9% pure. ^{1}H NMR (D_2O, 400 MHz): δ 1.02-1.22 (m, 2H, C*H*$_2$CH$_2$NH$_{arginine}$), 1.42-1.52 (m, 1H of the C*H*$_2$CH$_{arginine}$), 1.59-1.69 (m, 1H of the C*H*$_2$CH$_{arginine}$), 2.99 (dd, *J* = 13.4 Hz, *J'* = 10.3 Hz, 1H of the C*H*$_2$-β$_{tyrosine}$), 3.02-3.05 (m, 2H, C*H*$_2$-β$_{arginine}$), 3.22 (dd, *J* = 13.4 Hz, *J'* = 5.8 Hz, 1H of the C*H*$_2$-β$_{tyrosine}$), 4.08 (dd, *J* = 9.6 Hz, *J'* = 4.5 Hz, 1H, C*H*-α$_{arginine}$), 4.18 (dd, *J* = 10.3 Hz, *J'* = 5.8 Hz, 1H, C*H*-α$_{tyrosine}$), 6.88 (d, *J* = 8.5 Hz, 2H, C*H*$_{aryl}$), 7.15 (d, *J* = 8.5 Hz, 2H, C*H*$_{aryl}$). MS (ESI) *m/z* = 337.1 $[M+H]^+$, 169.0 $[M+2H]^{2+}$.

KTP-NH_2-LD. By the general procedure, Fmoc-D-Arg(pmc)-OH (4 equiv) and Fmoc-Tyr(*t*Bu)-OH (4 equiv) provided H-Tyr-D-Arg-NH_2 (66 mg, 70%) as a colorless solid. HPLC (water/acetonitrile, 0.1% TFA, 2-100%, 17 min): retention time, 2.41 min; 99% pure. ^{1}H NMR (D_2O, 400 MHz): δ 1.00-1.19 (m, 2H, C*H*$_2$$CH_2NH_{arginine}$), 1.42-1.52 (m, 1H of the C*H*$_2$$CH_{arginine}$), 1.59-1.68 (m, 1H of the C*H*$_2$$CH_{arginine}$), 2.96 (dd, *J* = 13.3 Hz, *J'* = 10.3 Hz, 1H of the C*H*$_2$-$\beta_{tyrosine}$), 3.01-3.04 (m, 2H, C*H*$_2$-$\beta_{arginine}$), 3.21 (dd, *J* = 13.3 Hz, *J'* = 5.8 Hz, 1H of the C*H*$_2$-$\beta_{tyrosine}$), 4.06 (dd, *J* = 9.6 Hz, *J'* = 4.5 Hz, 1H, C*H*-$\alpha_{arginine}$), 4.17 (dd, *J* = 10.3 Hz, *J'* = 5.8 Hz, 1H, C*H*-$\alpha_{tyrosine}$), 6.87 (d, *J* = 8.5 Hz, 2H, C*H*$_{aryl}$), 7.14 (d, *J* = 8.5 Hz, 2H, C*H*$_{aryl}$). MS (ESI) *m/z* = 337.1 $[M+H]^+$, 169.0 $[M+2H]^{2+}$.

KTP-NH_2-DD. By the general procedure, Fmoc-D-Arg(pmc)-OH (4 equiv) and Fmoc-D-Tyr(*t*Bu)-OH (4 equiv) provided H-D-Tyr-D-Arg-NH_2 (75 mg, 80%) as a colorless solid. HPLC (water/acetonitrile, 0.1% TFA, 2-100%, 17 min): retention time, 1.52 min; 99.9% pure. ^{1}H NMR (D_2O, 400 MHz): δ 1.49-1.62 (m, 2H, C*H*$_2$$CH_2NH_{arginine}$), 1.65-1.86 (m, 2H, C*H*$_2$$CH_{arginine}$), 3.10-3.17 (m, 4H, C*H*$_2$-$\beta_{arginine}$ and C*H*$_2$-$\beta_{tyrosine}$), 4.20-4.26 (m, 2H, C*H*-$\alpha_{tyrosine}$ and C*H*-$\alpha_{arginine}$), 6.85 (d, *J* = 8.4 Hz, 2H, C*H*$_{aryl}$), 7.13 (d, *J* = 8.4 Hz, 2H, C*H*$_{aryl}$). MS (ESI) *m/z* = 337.1 $[M+H]^+$, 169.0 $[M+2H]^{2+}$.

Me-KTP-NH_2-LD. By the general procedure, Fmoc-D-Arg(pmc)-OH (4 equiv) and Fmoc-N-Me-Tyr(*t*Bu)-OH (4 equiv) provided *N*-Me-Tyr-D-Arg-NH_2 (58 mg, 60%) as a colorless solid. HPLC (water/acetonitrile, 0.1% TFA, 2-100%, 17 min): retention time, 2.29 min; 97.7% pure. ^{1}H NMR (D_2O, 400 MHz): δ 0.98-1.18 (m, 2H, C*H*$_2$$CH_2NH_{arginine}$), 1.39-1.49 (m, 1H of the C*H*$_2$$CH_{arginine}$), 1.56-1.65 (m, 1H of the

C*H*$_2$CH$_{arginine}$), 2.73 (s, 3H, NC*H*$_3$), 2.94 (dd, *J* = 13.1 Hz, *J'* = 11.0 Hz, 1H of the C*H*$_2$-$\beta_{tyrosine}$), 2.99-3.04 (m, 2H, C*H*$_2$-$\beta_{arginine}$), 3.30 (dd, *J* = 13.1 Hz, *J'* = 5.3 Hz, 1H of the C*H*$_2$-$\beta_{tyrosine}$), 4.04 (dd, *J* = 9.8 Hz, *J'* = 4.6 Hz, 1H, C*H*-$\alpha_{arginine}$), 4.07 (dd, *J* = 11.0 Hz, *J'* = 5.3 Hz, 1H, C*H*-$\alpha_{tyrosine}$), 6.87 (d, *J* = 8.5 Hz, 2H, C*H*$_{aryl}$), 7.13 (d, *J* = 8.5 Hz, 2H, C*H*$_{aryl}$). MS (ESI) *m/z* = 351.1 $[M+H]^+$, 176.0 $[M+2H]^{2+}$.

Me-KTP-NH2. By the general procedure, Fmoc-Arg(pmc)-OH (4 equiv) and Fmoc-N-Me-Tyr(*t*Bu)-OH (4 equiv) provided *N*-Me-Tyr-Arg-NH$_2$ (56 mg, 58%) as a colorless solid. HPLC (water/acetonitrile, 0.1% TFA, 2-100%, 17 min): retention time, 1.66 min; 98.7% pure. ^{1}H NMR (D$_2$O, 400 MHz): δ 1.50-1.58 (m, 2H, C*H*$_2$CH$_2$NH$_{arginine}$), 1.63-1.70 (m, 1H of the C*H*$_2$CH$_{arginine}$), 1.72-1.80 (m, 1H of the C*H*$_2$CH$_{arginine}$), 2.71 (s, 3H, NC*H*$_3$), 3.06 (dd, *J* = 13.8 Hz, *J'* = 9.0 Hz, 1H of the C*H*$_2$-$\beta_{tyrosine}$), 3.17 (t, 2H, *J* = 6.9 Hz, C*H*$_2$-$\beta_{arginine}$), 3.20 (dd, *J* = 13.8 Hz, *J'* = 5.7 Hz, 1H of the C*H*$_2$-$\beta_{tyrosine}$), 4.12 (dd, *J* = 9.0 Hz, *J'* = 5.7 Hz, 1H, C*H*-$\alpha_{tyrosine}$), 4.42 (dd, *J* = 7.8 Hz, *J'* = 6.8 Hz, 1H, C*H*-$\alpha_{arginine}$), 6.86 (d, *J* = 8.5 Hz, 2H, C*H*$_{aryl}$), 7.12 (d, *J* = 8.5 Hz, 2H, C*H*$_{aryl}$). MS (ESI) *m/z* = 351.1 $[M+H]^+$, 176.0 $[M+2H]^{2+}$.

5.1.2. Solution phase synthesis of peptides KTP-NH$_2$-DL, Me-KTP-NH$_2$-LD and Me-KTP-NH$_2$

General procedure for the coupling reaction between tyrosine and arginine derivatives. NMM (3 equiv, 30 mmol) was added to a solution of tyrosine derivative (1 equiv, 10 mmol) in DMF (40 mL), and the resulting mixture was stirred at room temperature for 1 h. Then, BOP (1 equiv, 10 mmol) and arginine derivative (1.05 equiv, 10.5 mmol) were added. The resulting reaction mixture was stirred overnight at room temperature. Upon completion of the reaction (HPLC monitoring), the reaction mixture was filtered. The

resulting solution was diluted with ethyl acetate (100 mL), washed with saturated sodium bicarbonate (3 x 50 mL), water (100 mL), 1M aqueous potassium hydrogensulfate (3 x 50 mL), and brine (50 mL). The organic layer was dried over magnesium sulfate, filtered and concentrated under reduced pressure. The crude material was triturated with *n*-pentane, filtered, washed with *n*-pentane and dried to obtain the expected peptides which were used in the next step without further purification.

Synthesis of Boc-D-Tyr(Bzl)-Arg-NH_2. By the general procedure, Boc-D-Tyr(Bzl)-OH (3.71 g, 10 mmol) and H-D-Arg-NH_2 2HCl (2.58 g, 10 mmol) provided Boc-D-Tyr(Bzl)-Arg-NH_2 (3.15 g, 60%) as a colorless solid. ^{1}H-NMR (DMSO-d_6 + a drop D_2O, 400 MHz): δ 1.19-1.28 (m, 2H of the CH_2CH_2N$H_{arginine}$), 1.28 (s, 9H, (CCH_3)$_3$), 1.37-1.43 (m, 1H of the CH_2C$H_{arginine}$), 1.68-1.70 (m, 1H of the CH_2C$H_{arginine}$), 2.68 (dd, *J* = 13.6 Hz, *J'* = 9.2 Hz, 1H of the CH_2-$\beta_{tyrosine}$), 2.82 (dd, *J* = 13.6 Hz, *J'* = 5.2 Hz, 1H of the CH_2-$\beta_{tyrosine}$), 2.99 ($t_{aparent}$, *J* = 6.8 Hz, 2H, CH_2-$\beta_{arginine}$), 4.06-4.11 (m, 2H, C*H*-$\alpha_{tyrosine}$ and C*H*-$\alpha_{arginine}$), 5.01 (s, 2H, CH_2O), 6.87 (d, *J* = 8.4 Hz, 2H, CH_{aryl}), 7.00 (d, *J* = 7.2 Hz, 1H, N*H*), 7.12 (d, *J* = 8.4 Hz, 2H, CH_{aryl}), 7.17 (br, 1H, N*H*), 7.29-7.40 (m, 5H, CH_{aryl}), 8.12 (d, *J* = 8.0 Hz, 1H, N*H*). ^{13}C NMR (DMSO-d_6, 100 MHz): δ 24.8 (t), 28.2 (q, 3C), 28.9 (t), 36.3 (t), 40.3 (t), 51.8 (d), 56.3 (d), 69.1 (t), 78.2 (s), 114.3 (d, 2C), 127.6 (d, 2C), 127.7 (d), 128.4 (d, 2C), 130.0 (s), 130.2 (d, 2C), 137.2 (s), 155.6 (s), 156.7 (s), 156.9 (s), 171.8 (s), 173.3 (s). HRMS (ESI) *m/z* calcd. for $C_{27}H_{39}N_6O_5$ $[M+H]^+$ 527.2976, found 527.3005. HPLC (water/acetonitrile, 0.1% TFA, 2-100%, 17 min): retention time, 7.45 min; 99.9% pure.

Synthesis of Boc-N-Me-Tyr(Bzl)-D-Arg-NH_2. By the general procedure, Boc-N-Me-Tyr(Bzl)-OH (3.85 g, 10 mmol) and H-D-Arg-NH_2 2HCl (2.58 g, 10.5 mmol) provided Boc-N-Me-Tyr(Bzl)-D-Arg-NH_2 (4.86 g, 90%) as a colorless solid. ^{1}H NMR (DMSO-d_6, 400 MHz, 110 ºC): δ 1.34 (s, 9H, (CCH_3)$_3$), 1.46-1.53 (m, 2H, CH_2CH$_2$NH$_{arginine}$), 1.55-1.63 (m, 1H of the CH_2CH$_{arginine}$), 1.72-1.81 (m, 1H of the CH_2CH$_{arginine}$), 2.69 (s, 3H, NCH_3), 2.83 (m, 1H of the CH_2-β$_{tyrosine}$), 3.10-3.14 (m, 3H, CH_2-β$_{arginine}$ and 1H of the CH_2-β$_{tyrosine}$), 4.25-4.30 (m, 1H, CH-α$_{arginine}$), 4.69 (dd, J = 10.0 Hz, J' = 5.6 Hz, 1H, CH-α$_{tyrosine}$), 5.05 (s, 2H, CH_2O), 6.83 (br, 4H, NH), 6.90 (d, J = 8.4 Hz, 2H, CH_{aryl}), 7.10 (d, J = 8.4 Hz, 2H, CH_{aryl}), 7.28-7.40 (m, 5H, CH_{aryl}). ^{13}C NMR (DMSO-d_6, 100 MHz, 80 ºC): δ 24.5 (t), 27.5 (q, 3C), 28.7 (t), 30.6 (q), 33.2 (t), 40.1 (t), 51.5 (d), 59.7 (d), 69.2 (t), 78.7 (s), 114.4 (d, 2C), 126.9 (d, 2C), 127.1 (d), 127.8 (d, 2C), 129.4 (d, 2C), 129.9 (s), 136.9 (s), 154.6 (s), 156.7 (s), 156.9 (s), 169.7 (s), 172.6 (s). HRMS (ESI) *m/z* calcd. for $C_{28}H_{41}N_6O_5$ $[M+H]^+$ 541.3133, found 541.3151. HPLC (water/acetonitrile, 0.1% TFA, 2-100%, 17 min): retention time, 7.68 min; 99.9% pure.

Synthesis of Boc-N-Me-Tyr(Bzl)-Arg-NH_2. By the general procedure, Boc-N-Me-Tyr(Bzl)-OH (3.85 g, 10 mmol) and H-Arg-NH_2 2HCl (2.58 g, 10.5 mmol) provided Boc-N-Me-Tyr(Bzl)-D-Arg-NH_2 (4.91 g, 91%) as a colorless solid. ^{1}H NMR (DMSO-d_6, 400 MHz, 80ºC): δ 1.32 (s, 9H, (CCH_3)$_3$), 1.46-1.58 (m, 2H, CH_2CH$_2$NH$_{arginine}$), 1.60-1.64 (m, 1H of the CH_2CH$_{arginine}$), 1.75-1.83 (m, 1H of the CH_2CH$_{arginine}$), 2.70 (s, 3H, NCH_3), 2.85 (dd, J = 14.4 Hz, J' = 10.4 Hz, 1H of the CH_2-β$_{tyrosine}$), 3.11-3.17 (m, 4H, CH_2-β$_{arginine}$, 1H of the CH_2-β$_{tyrosine}$ and CH-α$_{tyrosine}$), 4.25-4.30 (m, 1H, CH-α$_{arginine}$), 5.07 (s, 2H, CH_2O), 6.91 (d, J = 8.6 Hz, 2H, CH_{aryl}), 6.85 (br, 5H, NH), 7.14 (d, J = 8.6 Hz, 2H, CH_{aryl}), 7.30-7.43 (m, 3H, CH_{aryl}), 7.49-7.51 (m, 2H, CH_{aryl}). ^{13}C NMR (DMSO-d_6, 100 MHz, 80 ºC): δ 24.6 (t), 27.6 (q, 3C), 28.9 (t), 30.5 (q), 33.0 (t),

40.1 (t), 51.7 (d), 59.5 (d), 69.2 (t), 78.7 (s), 114.4 (d, 2C), 126.9 (d, 2C), 127.2 (d), 127.9 (d, 2C), 129.3 (d, 2C), 129.9 (s), 136.9 (s), 154.6 (s), 156.68 (s), 156.72 (s), 169.8 (s), 172.6 (s). HRMS (ESI) *m/z* calcd. for $C_{28}H_{41}N_6O_5$ $[M+H]^+$ 541.3133, found 541.3150. HPLC (water/acetonitrile, 0.1% TFA, 2-100%, 17 min): retention time, 7.62 min; 99.9% pure.

General procedure for the removal of OBzl and N-Boc groups. The corresponding protected peptides (1 equiv) were dissolved in 50 mL of EtOH in a 100 mL two-neck round bottom flask. Pd/C (10 mol%) was added to the solution and the mixture was degassed twice under vacuum (using a water pump) and was replacing each time the vacuum by hydrogen (H_2 balloon). Next, the reaction mixture was permitted to react at room temperature under a hydrogen flow (H_2 balloon). After completion of the reaction (HPLC monitoring), the mixture was filtered through a Celite® bed to remove Pd/C, and the filtrate was evaporated *in vacuo*. The crude product was then dissolved in 50 mL of HCl 4M in 1,4-dioxane and stirred at room temperature. After completion of the reaction (HPLC monitoring), the resulting precipitate was collected by filtration, washed with 1,4-dioxane (2 x 10 mL), diethyl ether (2 x 10 mL) and *n*-pentane (2 x 10 mL) and dried in *vacuo*. The resulting white solid was dissolved in water and lyophylized to afford the corresponding deprotected dipeptides.

Synthesis of KTP-NH_2-DL. By the general procedure, Boc-D-Tyr(Bzl)-Arg-NH_2 (2.89 g, 5.5 mmol) provided H-D-Tyr-Arg-NH_2 (1.31 g, 71%) as a colorless solid. ^{1}H-NMR (D_2O, 400 MHz): as describe above. ^{13}C NMR (D_2O, 100 MHz): δ 27.2 (t), 30.9 (t), 39.0 (t), 43.3 (t), 56.2 (d), 57.5 (d), 118.7 (d, 2C), 128.6 (s), 133.6 (d, 2C), 158.1 (s), 159.6 (s), 172.3 (s), 178.8 (s). HRMS (ESI) *m/z* calcd. for $C_{15}H_{25}N_6O_3$ $[M+H]^+$

337.1983, found 337.1988. HPLC (water/acetonitrile, 0.1% TFA, 2-100%, 17 min): retention time, 2.36 min; 99.9% pure.

Synthesis of Me-KTP-NH_2-LD. By the general procedure, Boc-N-Me-Tyr(Bzl)-D-Arg-NH_2 (4.32 g, 8.0 mmol) provided N-Me-Tyr-D-Arg-NH_2 (1.71 g, 61%) as a colorless solid. ^{1}H-NMR (D_2O, 400 MHz): as describe above. ^{13}C NMR (D_2O, 100 MHz): δ 27.2 (t), 30.8 (t), 34.4 (q), 38.0 (t), 43.3 (t), 56.4 (d), 65.7 (d), 118.7 (d, 2C), 128.2 (s), 133.6 (d, 2C), 158.1 (s), 159.6 (s), 171.1 (s), 178.6 (s). HRMS (ESI) *m/z* calcd. for $C_{16}H_{26}N_6NaO_3$ $[M+Na]^+$ 373.1959, found 373.1961; calcd. for $C_{16}H_{27}N_6O_3$ $[M+H]^+$ 351.2139, found 351.2154. HPLC (water/acetonitrile, 0.1% TFA, 2-100%, 17 min): retention time, 2.29 min; 99.0% pure.

Synthesis of Me-KTP-NH_2. By the general procedure, Boc-N-Me-Tyr(Bzl)-Arg-NH_2 (4.32 g, 8.0 mmol) provided N-Me-Tyr-Arg-NH_2 (2.24 g, 81%) as a colorless solid. ^{1}H-NMR (D_2O, 400 MHz): as describe above. ^{13}C NMR (D_2O, 100 MHz): δ 27.2 (t), 31.1 (t), 34.6 (q), 38.2 (t), 43.4 (t), 56.1 (d), 65.6 (d), 118.8 (d, 2C), 127.8 (s), 133.7 (d, 2C), 158.1 (s), 159.6 (s), 170.6 (s), 177.5 (s). HRMS (ESI) *m/z* calcd. for $C_{16}H_{27}N_6O_3$ $[M+H]^+$ 351.2139, found 351.2139. HPLC (water/acetonitrile, 0.1% TFA, 2-100%, 17 min): retention time, 1.66 min; 99.0% pure.

5.2. Animals

For the sake of the 3R´s policy on animal experimentation, a preliminary screening test was performed to reduce the number of compounds to be tested. Given the number of tests and replicates, each drug lead to be withdrawn from the study impacts significantly on the number of animals to be manipulated and sacrificed. Three lead compounds were

selected from in vitro determination of the affinity of the compounds to anionic lipid membranes: Me-KTP-NH_2, Me-KTP-NH_2-LD, and KTP-NH_2-DL; Me stands for methylation at the N terminus and D refers to the use of a D-Tyr residue (DL) or a D-Arg residue (LD). Data on KTP-NH_2 was published before[10, 15] and used for comparison.

5.2.1. Mice

Male Swiss mice (4-6 weeks old) were obtained from a colony at Butantan Institute, São Paulo, Brazil. Animals were maintained in sterile microisolator cages with sterile rodent feed and acidified water ad libitum, and housed in positive-pressure air-conditioned units (25°C, 50% relative humidity) on a 12 h light/dark cycle. All procedures were performed in accordance with the guidelines provided by the Brazilian College of Animal Experimentation.

5.2.2 Rats

Adult male Wistar rats (Charles River, L'Arbresle, France), weighing between 210 and 250 g, were housed in groups at temperature and light-controlled conditions (22±2 ºC; lights on between 7:00 a.m. and 7:00 p.m.), with free access to food and water. In order to induce habituation to the researcher and to minimize stress, the animals were gently handled daily in the test room and hot-plate device during 4 days prior to nociceptive evaluation. At the day of experiments, animals were brought to the same room for at least 2h before testing. All experiments were performed in accordance with the European Directive 2010/63/EU. The project was approved by the institutional Animal Welfare Body (ORBEA-IMM) and licensed by DGAV (Direcção Geral de Veterinária) – the Portuguese competent authority for animal welfare.

5.3. Intravital microscopy

The dynamics of alterations in the microcirculatory network were determined using intravital microscopy (IVM), a light microscopy-based approach that enables imaging subcellular structures in live animals. Endothelial cells can actively regulate the migration of leukocytes through the vessel wall by expressing adhesion molecules and chemokines on their luminal surface, allowing leukocytes to adhere and finally migrate into the tissue. The cremaster muscle was used as the principal tissue for analysis of leukocyte–vessel wall interactions because of its thin and transparent nature. IVM was conducted on an upright microscope (Axiolab, Carl Zeiss, Oberkochen, Germany) coupled to a digital camera for image acquisition (AxioCam Icc1, Carl Zeiss, Oberkochen, Germany).

5.3.1. Cremaster muscle preparation

Mice were injected ip with a muscle relaxant drug (0.4% xylazine) (Calmiun®, Agner União, São Paulo, Brazil) and after 5 min anesthetized with 0.5 g/Kg of ketamine (Holliday-Scott SA, Buenos Aires, Argentina) ip. Animals were placed on a 37ºC heating pad and the microsurgery was performed as described previously.[30] Briefly, the scrotum was opened and the cremaster muscle exteriorized. A longitudinal incision on the muscle allowed its exposure to full access to the microcirculatory network. Post-capillary venules were measured with Axiovision program v 4.8.2.0, and one venule ranging between 25-40 μm of diameter in each animal was chosen to count the number of rolling leukocytes.

5.3.2. Leukocyte recruitment measurements[31]

After stabilization of the microcirculation, the number of rolling and adherent leukocytes in the postcapillary venules were counted every 10 min, up to 30 min, after peptide topical application. A leukocyte was considered to be adhering to the venular endothelium if it remained stationary for 60 s or longer at a pre-set distance of 100 μM. A rolling leukocyte was defined as a white cell that moved slower than the stream of flowing erythrocytes. The number of rolling leukocytes was quantified as the number of white cells that passed a fixed pre-set point during 1 min.

5.3.3. Experimental Protocol for IVM

Initially, cremaster muscles of mice were topically applied with 20 μL of KTP-NH_2-DL, Me-KTP-NH_2, or Me-KTP-NH_2-LD at 48 or 96 μM for visualization of their capacity to induce mobilization of leukocytes along the vessel wall. Sterile phosphate-buffered saline (PBS, pH 7.4) was used as control.

For investigation of the anti-inflammatory effect of KTP-NH_2-DL, mice were pretreated with an ip injection of LPS at 0.05 μg/kg (E. coli 055:B5, Sigma) dissolved in sterile saline. 30 min after ip administration of LPS, cremaster muscles of mice were exposed to a topic application of 20 μL of KTP-NH_2-DL at 96 μM. Negative-control mice were pretreated with ip injection of sterile saline and submitted to topic application of sterile PBS. Positive-control mice were pretreated with ip injection of LPS and submitted to topic application of sterile PBS.

5.4. Evaluation of thermal nociceptive responses in the hot-plate test[32]

The hot plate test consisted in evaluation of animal behavioral responses to noxious thermal stimulus, such as hind-paw withdrawal and/or shaking.[33] The hot plate test is frequently elected to evaluate behavioral responses to acute nociceptive stimulation and

has the advantage over other acute behavioral tests of depending on central processing and not being a simple spinal reflex.[32] The hot plate test is frequently the only acute behavioral test used to predict the analgesic efficacy of new drugs.[34-37] Based on these reasons and in order to allow comparisons of the results of the present study with our previous reports with KTP derivatives[10, 17], the hot plate test was elected. Animals were placed inside a transparent glass box (20.5x10 cm; 20 cm height) on the metallic surface of the hot plate apparatus (IITC Incremental Hot/Cold plate, Series 8/Software, IITC Life San Fernando Valley, CA, USA). The initial temperature was 35.2°C, and an increasing rate temperature of 9°C per minute was defined (cut-off at 52,5ºC). The temperature to elicit a pain behavior was recorded. A cut-off temperature of 52.5°C was defined. Animals ($n \geq 5$ per group) were evaluated before Me-KTP-NH_2, Me-KTP-NH_2-LD, KTP-NH_2-DL or saline injection (basal values) and 15, 30, 45, 60, 75 and 90 min after ip injections. The responses are shown as the difference between values at each time point after injection and the respective basal values (at time zero). This is a solid procedure which allows that the response of each animal is analyzed and compared with the respective baseline values along the time.[10, 17, 38] Data are represented as the group means ± SEM. The significance of differences in each group was analyzed with two way ANOVA followed by Tukey's post hoc test (section 5.6).

5.5. Permeation studies

Permeation studies were performed in a 24-well transwell permeable supports. They were carried out for 18 h and were performed in triplicate. The basal compartment was filled with 800 μL of 4-(2-hydroxyethyl)-1-piperazineethanesulfonic acid (HEPES, pH 7.4) buffer and the apical compartment loaded with 200 μL of the drug solution. The

apical compartment was placed on top of the base being separated by a filter with or without lipid (sample versus blank filter). The apparatus were then incubated at 25ºC in an orbital shaker at 100 rpm for different time intervals. After incubation, the apparatus was disassembled and the basal and apical solutions were kept at 4ºC until use. Samples were transferred to standard 10 mm path length quartz cuvettes and the fluorescence emission intensity was measured in a spectrofluorimeter (FS920, Edinburgh Instruments, Livingston, UK), at room temperature. The spectroscopic experiments were as described elsewhere.[17] After permeation assays, the samples were diluted to an absorbance bellow 0.1 at the excitation wavelength to minimize inner filter effects.[39] The dose tested was based on a previous study showing that the analgesic dose of KTP-NH_2, 32.3 $mg \cdot kg^{-1}$ = 96 μM, was efficient in all pain models tested.[10] Thus, stock solutions of KTP-NH_2 isomers and KTP were prepared by dissolving in HEPES buffer to a final apical concentration of 1.6 mM.

5.5.1. Relative permeability calculation

The fluorescence intensity of the drug at the apical compartment was plotted against time and the slope, m, of the linear part of the curves (approximate steady-state flux rate) at t=0 was calculated for both samples (filter + lipid bilayers' stack) and blank filters (i.e. in the absence of lipid). Sample permeability (Ps) and blank permeability (Pb) may be simply calculated according to:[11]

$$P_x = m_x \cdot \frac{V}{A} \qquad (2)$$

where x refers to sample (s) or blank (b), V is the basal volume, and A the area of the filter. Experimentally the relative permeability (P_R) reads:

$$P_R = \frac{P_s}{P_b} = \frac{m_s}{m_b} \quad (3)$$

P_R was calculated considering the first 10 hours, during which it was observed an approximate linear regime for the majority of drugs (Supporting information).

5.5.2. Preparation of lipid barriers

The preparation of the lipid barrier was described elsewhere.[19] Shortly, small unilamellar vesicles (SUVs) of 1-palmitoyl-2-oleoyl-sn-glycero-3-phosphocholine (POPC) were prepared. The deposited lipid film was hydrated with HEPES buffer to a final concentration of 5 mM. The lipid was then homogenized by 8 cycles of freeze-thawing and dissolved with HEPES buffer to a final concentration of 1 mM. SUVs were obtained by sonication with a tip sonicator (Vibra cell – Sonics & Material Inc, Danbury Connecticut, USA) operated in a continuous mode for 15 min with refrigeration, followed by centrifugation (Eppendorf centrifuge) at maximum speed for 30 min to remove titanium particles.

100 μL of the vesicular suspension was deposited to each culture insert in the transwells (0.4 μm pore size, 0.33 cm^2 area), and 10 mM of $CaCl_2$ was added to promote the formation of fused vesicles. The inserts were placed into 24-wells culture plate, and centrifuged at 693 × g (2000 rpm) (Multifuge 1L-R, Heraeus, Germany) for 4 min, at room temperature. The inserts were then placed in fresh wells, and 100 μL of the vesicular suspension were again added to the filters followed by centrifugation at the same speed for 10 min. To improve lipid dispersion in the filter area, the plates were rotated 180 ºC between centrifugations. The inserts were placed in a new plate and incubated at 50 ºC for 25 min. After 5 min at room temperature, 100 μL of the liposomal suspension were added to the filters and centrifuged for 30 min. Few filters

did not hold the lipid suspension and were excluded from the experiment.[40] The remaining filters were carefully inverted to discard the supernatant. Thereafter, the filters were froze/thawed at -80 ºC for 1 h and 65 ºC for 30 min, followed by incubation overnight at 4 ºC until permeation studies.

5.6. Statistical analyses

Data are represented as mean ± SEM. Statistically differences were analyzed by one-way or two-way ANOVA followed by Tukey's post test. Differences were considered significant when $p < 0.05$. $p < 0.01$ and $p < 0.001$ are also mentioned where applicable for the sake of completeness of the results. All statistical analyses were calculated with Prism 6 software (GraphPad Software, version 6.02).

6. ASSOCIATED CONTENT

6.1. Supporting Information

NMR (^{1}H, ^{13}C, COSY dept) and HRMS for all new compounds. HPLC of final compounds.
Measure of relative permeability in permeation studies.

7. AUTHOR INFORMATION

7.1. **Corresponding Authors**

For K.C.: E-mail, katia.conceicao@unifesp.br

For M.A.R.B.C.: E-mail, macastanho@medicina.ulisboa.pt

7.2. **Author Contributions**

* K.C. and M.A.R.B.C. contributed equally to this work

7.3. Notes

The authors declare no competing financial interest.

8. ACKNOWLEDGEMENTS

FCT-MCTES is acknowledged for PhD fellowship SFRH/BD/52225/2013 to Juliana Perazzo. Marie Skłodowska-Curie Research and Innovation Staff Exchange (RISE) is acknowledged for funding: call H2020-MSCA-RISE-2014, Grant agreement 644167, 2015-2019. The authors thank Dr. Marta Ribeiro for lipid affinity and plasma stability studies and Dr. Ricardo Pinheiro for participation in the chemical syntheses.

9. ABBREVIATIONS USED

BOP, benzotriazole-1-yl-oxy-tris-(dimethylamino)-phosphonium hexafluorophosphate; Bzl, benzyl; DIEA, diisopropylethylamine; HBTU, *O*-(benzotriazol-1-yl)-*N*,*N*,*N'*,*N'*-tetramethyluronium hexafluorophosphate; HCl, hydrochloric acid; HEPES, 4-(2-hydroxyethyl)-1-piperazineethanesulfonic acid; HOBt, *N*-hydroxybenzotriazole; IVM, intravital microscopy; KTP, kyotorphin; KTP-NH_2, amidated KTP; LPS, lipopolysaccharide; MD2, myeloid differentiation protein 2; NMM, *N*-methylmorpholine; PEPT2, peptide transporter 2; PLC, phospholipase C; pmc, 2,2,5,7,8-pentamethyl-chroman-6-sulfonyl; P_R, relative permeability; SUVs, small unilamellar vesicles; TIS, triisopropylsilane.

10. REFERENCES

1. Takagi, H.; Shiomi, H.; Ueda, H.; Amano, H. A novel analgesic dipeptide from bovine brain is a possible Met-enkephalin releaser. *Nature* **1979,** *282* (5737), 410-412.

2. Takagi, H.; Shiomi, H.; Ueda, H.; Amano, H. Morphine-like analgesia by a new dipeptide, L-tyrosyl-L-arginine (kyotorphin) and its analogue. *Eur. J. Pharmacol.* **1979,** *55* (1), 109-111.

3. Ueda, H.; Tatsumi, K.; Shiomi, H.; Takagi, H. Analgesic dipeptide, kyotorphin (tyr-arg), is highly concentrated in the synaptosomal fraction of the rat brain. *Brain Res.* **1982,** *231* (1), 222-224.

4. Shiomi, H.; Ueda, H.; Takagi, H. Isolation and identification of an analgesic opioid dipeptide kyotorphin (tyr-arg) from bovine brain. *Neuropharmacology* **1981,** *20* (7), 633-638.

5. Chen, P.; Bodor, N.; Wu, W. M.; Prokai, L. Strategies to target kyotorphin analogues to the brain. *J. Med. Chem.* **1998,** *41* (20), 3773-3781.

6. Kawabata, A.; Umeda, N.; Takagi, H. L-arginine exerts a dual role in nociceptive processing in the brain: Involvement of the kyotorphin-Met-enkephalin pathway and NO-cyclic GMP pathway. *Br. J. Pharmacol.* **1993,** *109* (1), 73-79.

7. Shiomi, H.; Kuraishi, Y.; Ueda, H.; Harada, Y.; Amano, H.; Takagi, H. Mechanism of kyotorphin-induced release of Met-enkephalin from guinea pig striatum and spinal cord. *Brain Res.* **1981,** *221* (1), 161-169.

8. Kolaeva, S. G.; Semenova, T. P.; Santalova, I. M.; Moshkov, D. A.; Anoshkina, I. A.; Golozubova, V. Effects of L-thyrosyl-L-arginine (kyotorphin) on the behavior of rats and goldfish. *Peptides* **2000,** *21* (9), 1331-1336.

9. Inoue, M.; Nakayamada, H.; Tokuyama, S.; Ueda, H. Peripheral non-opioid analgesic effects of kyotorphin in mice. *Neurosci. Lett.* **1997,** *236* (1), 60-62.

10. Ribeiro, M. M.; Pinto, A.; Pinto, M.; Heras, M.; Martins, I.; Correia, A.; Bardaji, E.; Tavares, I.; Castanho, M. Inhibition of nociceptive responses after systemic administration of amidated kyotorphin. *Br. J. Pharmacol.* **2011,** *163* (5), 964-973.

11. D. Serrano, I.; M. Freire, J.; V. Carvalho, M.; Neves, M.; N. Melo, M.; A.R.B. Castanho, M. The mechanisms and quantification of the selective permeability in transport across biological barriers: The example of kyotorphin. *Mini Rev. Med. Chem.* **2014,** *14* (2), 99-110.

12. Santos, S. M.; Garcia-Nimo, L.; Sa Santos, S.; Tavares, I.; Cocho, J. A.; Castanho, M. A. Neuropeptide kyotorphin (tyrosyl-arginine) has decreased levels in the cerebro-spinal fluid of Alzheimer's disease patients: Potential diagnostic and pharmacological implications. *Front. Aging Neurosci.* **2013,** *5*:68.

13. Sá Santos, S.; Santos, S. M.; Pinto, A. R.; Ramu, V. G.; Heras, M.; Bardaji, E.; Tavares, I.; Castanho, M. Amidated and ibuprofen-conjugated kyotorphins promote neuronal rescue and memory recovery in cerebral hypoperfusion dementia model. *Front. Aging Neurosci.* **2016,** *8:1*.

14. de la Torre, J. C.; Stefano, G. B. Evidence that Alzheimer's disease is a microvascular disorder: The role of constitutive nitric oxide. *Brain Res. Rev.* **2000,** *34* (3), 119-136.

15. Conceição, K.; Magalhães, P. R.; Campos, S. R.; Domingues, M. M.; Ramu, V. G.; Michalek, M.; Bertani, P.; Baptista, A. M.; Heras, M.; Bardaji, E. R.; Bechinger, B.; Ferreira, M. L.; Castanho, M. A. The anti-inflammatory action of the analgesic kyotorphin neuropeptide derivatives: Insights of a lipid-mediated mechanism. *Amino Acids* **2015,** 48 (1), 307-318.

16. Ribeiro, M. M.; Santos, S. S.; Sousa, D. S.; Oliveira, M.; Santos, S. M.; Heras, M.; Bardaji, E.; Tavares, I.; Castanho, M. A. Side-effects of analgesic kyotorphin derivatives: Advantages over clinical opioid drugs. *Amino Acids* **2013,** *45* (1), 171-178.

17. Ribeiro, M. M.; Pinto, A. R.; Domingues, M. M.; Serrano, I.; Heras, M.; Bardaji, E. R.; Tavares, I.; Castanho, M. A. Chemical conjugation of the neuropeptide kyotorphin and ibuprofen enhances brain targeting and analgesia. *Mol. Pharm.* **2011,** *8* (5), 1929-1940.

18. Ribeiro, M. M.; Domingues, M. M.; Freire, J. M.; Santos, N. C.; Castanho, M. A. Translocating the blood-brain barrier using electrostatics. *Front, Cell. Neurosci.* **2012,** *6*:44.

19. Serrano, I. D.; Ramu, V. G.; Pinto, A. R.; Freire, J. M.; Tavares, I.; Heras, M.; Bardaji, E. R.; Castanho, M. A. Correlation between membrane translocation and analgesic efficacy in kyotorphin derivatives. *Biopolymers* **2015,** *104* (1), 1-10.

20. Ramage, R.; Green, J.; Blake, A. J. An acid labile arginine derivative for peptide synthesis: NG-2,2,5,7,8-pentamethylchroman-6-sulphonyl-l-arginine. *Tetrahedron* **1991,** *47*, 6353-6370.

21. Fischer, P. M.; Retson, K. V.; Tyler, M. I.; Howden, M. E. Application of arylsulphonyl side-chain protected arginines in solid-phase peptide synthesis based on 9-fluorenylmethoxycarbonyl amino protecting strategy. *Int. J. Pept. Protein Res.* **1992,** *40* (1), 19-24.

22. Albericio, F.; Kneib-Cordonier, N.; Biancalana, S.; Gera, L.; Masada, R. I.; Hudson, D.; Barany, G. Preparation and application of the 5-(4-(9-fluorenylmethyloxycarbonyl)aminomethyl-3,5-dimethoxyphenoxy)-valeric acid (PAL) handle for the solid-phase synthesis of C-terminal peptide amides under mild conditions. *J. Org. Chem.* **1990,** *55* (12), 3730-3743.

23. Solé, N. A.; Barany, G. Optimization of solid-phase synthesis of [Ala8]-dynorphin-A. *J. Org. Chem.* **1992,** *57* (20), 5399-5403.

24. Atherton, A.; Born, G. V. R. Quantitative investigations of the adhesiveness of circulating polymorphonuclear leucocytes to blood vessel walls. *J. Physiol.* **1972,** *222* (2), 447-474.

25. Masedunskas, A.; Milberg, O.; Porat-Shliom, N.; Sramkova, M.; Wigand, T.; Amornphimoltham, P.; Weigert, R. Intravital microscopy: A practical guide on imaging intracellular structures in live animals. *Bioarchitecture* **2012,** *2* (5), 143-157.

26. Weigert, R.; Porat-Shliom, N.; Amornphimoltham, P. Imaging cell biology in live animals: Ready for prime time. *J. Cell Bio.* **2013,** *201* (7), 969-979.

27. Gavins, F. N. Intravital microscopy: New insights into cellular interactions. *Curr. Opin. Pharmacol.* **2012,** *12* (5), 601-607.

28. Ueda, H.; Yoshihara, Y.; Misawa, H.; Fukushima, N.; Katada, T.; Ui, M.; Takagi, H.; Satoh, M. The kyotorphin (tyrosine-arginine) receptor and a selective reconstitution with purified Gi, measured with GTPase and phospholipase C assays. *J. Biol. Chem.* **1989,** *264* (7), 3732-3741.

29. Vergnolle, N. Protease-activated receptors as drug targets in inflammation and pain. *Pharmacol. Ther.* **2009,** *123* (3), 292-309.

30. Lopes-Ferreira, M.; Moura-da-Silva, A. M.; Piran-Soares, A. A.; Angulo, Y.; Lomonte, B.; Gutierrez, J. M.; Farsky, S. H. Hemostatic effects induced by thalassophryne nattereri fish venom: A model of endothelium-mediated blood flow impairment. *Toxicon.* **2002,** *40* (8), 1141-147.

31. Sperandio, M.; Pickard, J.; Unnikrishnan, S.; Acton, S. T.; Ley, K. Analysis of leukocyte rolling in vivo and in vitro. *Methods Enzymo.* **2006,** *416*, 346-371.

32. Le Bars, D.; Gozariu, M.; Cadden, S. W. Animal models of nociception. *Pharmacol. Rev.* **2001,** *53* (4), 597-652.

33. Carter, R. B. Differentiating analgesic and non-analgesic drug activities on rat hot plate: Effect of behavioral endpoint. *Pain* **1991,** *47* (2), 211-220.

34. Craft, R. M.; Ulibarri, C.; Leitl, M. D.; Sumner, J. E. Dose- and time-dependent estradiol modulation of morphine antinociception in adult female rats. *Eur. J. Pain.* **2008,** *12* (4), 472-479.

35. Kline, R. H. t.; Wiley, R. G. Spinal mu-opioid receptor-expressing dorsal horn neurons: Role in nociception and morphine antinociception. *J. Neurosci.* **2008,** *28* (4), 904-913.

36. Li, X.; Shi, X.; Liang, D. Y.; Clark, J. D. Spinal CK2 regulates nociceptive signaling in models of inflammatory pain. *Pain* **2005,** *115* (1-2), 182-190.

37. Ruskin, D. N.; Kawamura, M.; Masino, S. A. Reduced pain and inflammation in juvenile and adult rats fed a ketogenic diet. *PloS one.* **2009,** *4* (12), e8349.

38. Martins, I.; Pinto, M.; Wilson, S. P.; Lima, D.; Tavares, I. Dynamic of migration of HSV-1 from a medullary pronociceptive centre: Antinociception by overexpression of the preproenkephalin transgene. *Eur. J. Neurosci.* **2008,** *28* (10), 2075-2083.

39. Lakowicz, J. R., *Principles of fluorescence spectroscopy*. Kluwer Academic/Plenum Publishers: New York, 1999.

40. Flaten, G. E.; Dhanikula, A. B.; Luthman, K.; Brandl, M. Drug permeability across a phospholipid vesicle based barrier: A novel approach for studying passive diffusion. *Eur. J. Pharm. Sci.* **2006,** *27* (1), 80-90.

Table of Contents Graphics